Fatigue behavior and lifetime prediction of unidirectionally wire reinforced lightweight metal matrix composites

Matthias Merzkirch, Thilo Hammers, Andreas Reeb, Thomas Schwind, Sascha Riedl, Leon Thiel, Alexander Henschel, Eberhard Kerscher, Volker Schulze, Kay A. Weidenmann

Angaben zur Veröffentlichung / Publication details:

Merzkirch, Matthias, Thilo Hammers, Andreas Reeb, Thomas Schwind, Sascha Riedl, Leon Thiel, Alexander Henschel, Eberhard Kerscher, Volker Schulze, and Kay A. Weidenmann. 2015. "Fatigue behavior and lifetime prediction of unidirectionally wire reinforced lightweight metal matrix composites." *Advanced Engineering Materials* 17 (6): 905–11. https://doi.org/10.1002/adem.201400354.

DOI: 10.1002/adem.201400354

Fatigue Behavior and Lifetime Prediction of Unidirectionally Wire Reinforced Lightweight Metal Matrix Composites**

By *Matthias Merzkirch,* Thilo Hammers, Andreas Reeb, Thomas Schwind, Sascha Riedl, Leon Thiel, Alexander Henschel, Eberhard Kerscher, Volker Schulze* and *Kay André Weidenmann*

In the field of lightweight construction for transportation means, hybrid structures composed of high-strength and low-density materials exhibit a high potential for application. The composite extrusion process allows an easy embedding of metallic reinforcements into a multitude of light metal alloys. The current work shows that different metallic wire reinforced light alloys with a content of 11.1 vol% lead to a significant increase in lifetime of different aluminum and magnesium alloys under fully reversed stress controlled fatigue loading. Based on the knowledge of the quasi-static behavior of the single components and the fatigue behavior of the matrix material, a new lifetime model is used to predict the lifetime for different unidirectionally reinforced material systems.

1. Introduction

The *composite extrusion* process, which is described in principle in ref.,[1] allows for a direct embedding of metallic wires and hybrid wires based on ceramic fibers[2–4] within lightweight metal matrices such as aluminum and magnesium alloys with the help of modified porthole dies. The current state of the art allows the production of a multitude of different continuous wire reinforced material combinations and profile geometries.[5] The maximum volume fraction of reinforcement the profiles is 13.5%[6] (see Figure 1) due to geometric and capacity restrictions of the extrusion press used within the Collaborative Research Center/Transregio 10 focussing on the production and characterization of this novel material class. Possible future applications can be found in the automotive and aerospace sectors.

Some basic investigations about the fatigue behavior of continuous fiber reinforced light metals have been done by Baker,[7] Moser *et al.*,[8] and Bettge *et al.*[9] on silica and steel fiber[7] as well as on alumina fiber[8] reinforced aluminum and aluminum alloys, whereas ref.[9] focussed on silicon carbide reinforced titanium.

The *damage behavior* of different unidirectionally monofilament, metallic wire, reinforced aluminium matrices under stress controlled cyclic loading has been studied in detail in refs.[10–17] It could be confirmed that the reinforcing element leads to a significant increase in lifetime, noticeable by a parallel shift of the regression lines of the *S–N* curves in double logarithmic scale. In refs.,[10–15] metallographic investigations proved that crack initiation starts from the outer matrix surface of EN AW-60xx and AZ31 reinforced with 11.1 vol% spring steel wire specimens. The cracks continued to grow until they reached the reinforcing element. The crack growth of metallic rope reinforced EN AW-6060[15] and spring steel wire reinforced EN AW-2099 and EN AW-6056[16,17] started from the interface between matrix and reinforcing element. A detailed view on the damage behavior under

[*] *M. Merzkirch, A. Reeb, V. Schulze, K. A. Weidenmann*
Institute for Applied Materials, Karlsruhe Institute of Technology (KIT), Engelbert-Arnold-Strasse 4, 76128, Karlsruhe, Germany
E-mail: matthias.merzkirch@kit.edu
T. Hammers
Hilti GmbH, 86916, Kaufering, Germany
T. Schwind
Hilti Corporation, 9494, Schaan, Liechtenstein
S. Riedl, L. Thiel
Airbus Group Astrium (Defence & Space) Im Langen Grund 1, 74239, Hardthausen am Kocher, Germany
A. Henschel, E. Kerscher
Materials Testing Group, University Kaiserslautern, 67663, Kaiserslautern, Germany

[**] *This paper is based on investigations of the subprojects A3–"Material systems for reinforced and functional extruded profiles" and T1–"Improved Properties of Aircraft Stringer Profiles by Composite Extrusion" of the Collaborative Research Center/Transregio 10, which is kindly supported by the German Research Foundation (DFG).*
The paper was modified 28th January 2015 after initial publication in Early View.

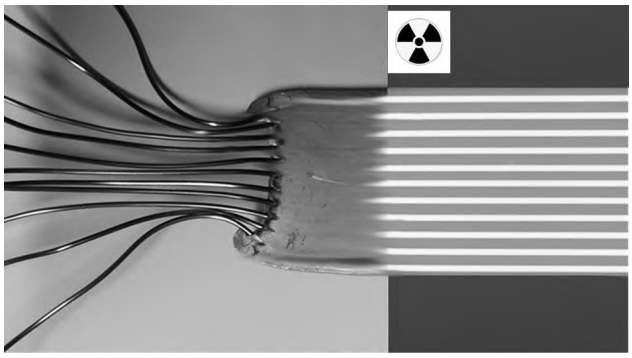

Fig. 1. Picture of the press start of an 48 × 3 mm² profile with 11 reinforcing elements (d = 15 mm) and a volume fraction of 13.5% (the right side depicts a CT investigation: the regular arrangement and good embedding into the matrix of the reinforcing elements).

fatigue loading of spring steel wire reinforced EN AW-6082 and AZ31 examined by means of the acoustic emission analysis has been given in refs.[10,12,14] In refs.,[10–12,14] altogether four stages of deformation and damage could be identified with the help of the evolution of the plastic strain amplitude and a damage parameter based on the loss in stiffness.[18] After strain hardening of the matrix material in stage I, stage II represents the (quasi) saturation stage. Within stage III, cracks initiate from the specimen's outer surface. Additionally to the crack growth within the matrix material, a debonding along the interface between wire and matrix could be confirmed after the cracks reach the reinforcing element. Subsequent to the failure of the matrix at the end of stage III, the reinforcing element starts to fatigue in stage IV after an initial strain hardening. The end of stage IV is characterized by the complete failure of the reinforcing element.

Figure 2 depicts the representative crack growth starting from the outer surface and along the interface (a) as well as the fracture of the matrix material and crack growth within the reinforcing element (b) (material system: EN AW-6082 + 301SS).[13,14]

The detailed deduction of a simple model for *lifetime prediction* of continuous fiber reinforced composites is presented in refs.[11,13,14] Based on the investigations done by Majumdar and Newaz[19] and Talreja[20] where the strain range controls fatigue life, the regression lines of the total strain amplitude $\epsilon_{t,a}$ shown in refs.[11,14,17] – which were derived from the strain response within the saturation state II (half fatigue life $N_f/2$) from the stress controlled S/N curves – plotted against the cycles to fracture in double logarithmic scale for both the unreinforced and the 11.1 vol% reinforced composite are within one scatter band. Consequently (in agreement to refs.),[19,20] it can be concluded that the fatigue life of the reinforced composite (C) is equal to the one of the unreinforced matrix material (M) for the measured total strain amplitudes $\epsilon_{t,a}$ (at the given stress amplitudes), which can be expressed by the following equation:

$$\epsilon_{t,a}(\sigma_{a,C}) = \epsilon_{t,a}(\sigma_{a,M}) \text{ if } N_f(C) = N_f(M) \tag{1}$$

and is analogous to the iso-strain model of Voigt.[21] $\sigma_{a,C}$ and $\sigma_{a,M}$ represent the stress amplitude for the composite and the matrix material, respectively.

In order to calculate the stress amplitude for the composite, assuming that the fatigue life for the unreinforced material is equal to the reinforced material at the same total strain amplitudes, the following expression can be expressed by Hooke's law:

$$\frac{\sigma_C}{E_C} = \frac{\sigma_M}{E_M} \Rightarrow \sigma_C = \sigma_M \cdot \frac{E_C}{E_M} \tag{2}$$

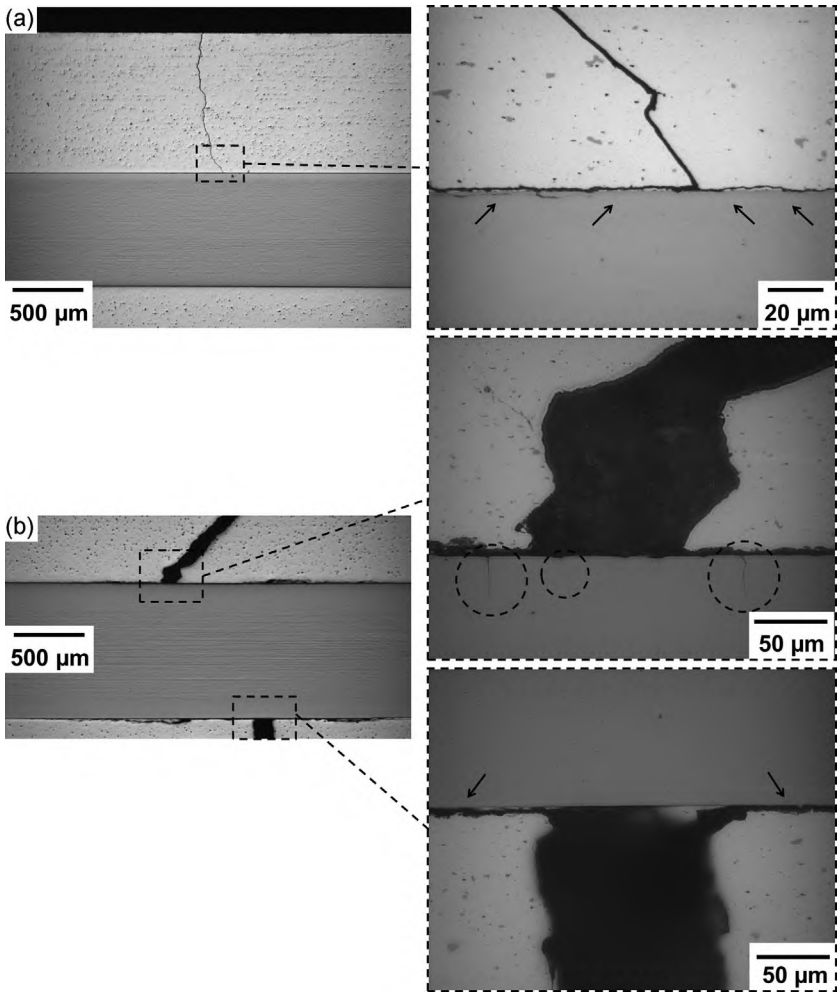

Fig. 2. Longitudinal sections of loaded composite specimens EN AW-6082 reinforced with 11.1 vol% spring steel wire (301SS) with zoom: prior to fracture of the matrix (stage III) (a) and after fracture of the matrix (stage IV) (b).[13,14]

By using the following equation – rule of mixture for the Young's modulus (where index RE represents the reinforcing element) in longitudinal direction:[21,22]

$$E_C = E_{RE} \cdot V_{RE} + E_M \cdot V_M \quad (3)$$

Equation (2) can be transformed to:

$$\sigma_C = \sigma_M \cdot \left(\frac{E_{RE}}{E_M} \cdot V_{RE} + (1 - V_{RE}) \right) \quad (4)$$

Based on the mechanical quasi-static data of the single components – E_{RE} and E_M represent the Young's moduli of the reinforcing element and the matrix, respectively, V_{RE} represents the volume fraction of reinforcement – and on the basis of the Basquin relation[23] for the matrix material's fatigue behavior, Equation (4) can be modified as follows:

$$\sigma_{a,C} = \left(\sigma'_{B,M} \cdot (N_f(M))^b \right) \cdot \left(\frac{E_{RE}}{E_M} \cdot V_{RE} + (1 - V_{RE}) \right) \quad (5)$$

The wide range of applicability of this lifetime model for different composite extruded material systems, which have been investigated within the Collaborative Research Center/Transregio 10 since 2003, will be presented in the current work. Besides the prediction of the fatigue lifetime of unidirectionally wire reinforced light metal alloys, the benefit of wire reinforcements for different metallic lightweight matrices will be discussed.

2. Materials

The profiles were manufactured on a 10 MN extrusion press at the Institute of Forming Technology and Lightweight Construction (IUL) at the Technical University of Dortmund. All reinforcing elements had a diameter of 1 mm. Generally, the composite profiles were manufactured from the same matrix material as the unreinforced profiles but were additionally reinforced during composite extrusion with the reinforcing elements.

The investigated materials were produced in several press runs in different profile geometries and therefore different press ratios. Table 1 lists the production parameters for the different material systems. In the following, a detailed labeling including the heat treatment states is presented. Details about the composition of the single constituents can be found in the given References.

Table 2 lists the materials used as matrix and as reinforcements and their Young's moduli measured during tensile tests in previously published contributions.

3. Specimen Geometry and Experimental Procedure

All specimens have been tested in longitudinal (extrusion) direction (LD). The gauge length of the cylindrical specimens was 10 mm with a diameter of 3 mm. The centrically placed wire had a diameter of 1 mm resulting in a volume fraction of $V_{RE} = 11.1\%$ in the gauge length.

The specimens were clamped using hydraulic grips. The load controlled fatigue tests were performed in environmental atmosphere at a stress ratio of $R = -1$ (fully reversed) and a sinusoidal loading. At least two specimens have been tested per load level and the maximum number of cycles until test end (run out) was chosen to be 10^7 cycles, which is defined as the endurance limit.

Since the current work involves the comparison of the results achieved in several studies,[10–17] Table 3 lists the

Table 1. Investigated material systems and production parameters.

Composite	Profile geometry	Press ratio	Ram speed in mm s^{-1}	Additional heat treatment after the extrusion process	Refs.
EN AW-2099 + Co	Z-profile	19:1	1	Solution annealed, quenched in water, stretch formed 2.5%, artificial ageing	[16,17,24]
EN AW-6056 + Fe	Z-profile	42:1	1	Solution annealed, quenched in water, stretch formed 0.6%, artificial ageing	[16,17,24]
EN AW-6060 + Haynes 25	40 × 10 mm²	42:1	1	Quenched with air, natural ageing	[15]
EN AW-6060 + 301SS	40 × 10 mm²	22:1	1	Quenched with air, natural ageing	[15]
EN AW-6082 + 301SS	40 × 10 mm²	19:1	1	Quenched with air, natural ageing	[13,14]
AZ31 + 301SS	40 × 10 mm²	19:1	1	Cooled in ambient air	[11]

Table 2. Materials used as reinforcement (left) and as matrix material (right) with their Young's moduli and ultimate tensile strengths.

Reinforcement	E [GPa]	σ_{UTS} [MPa]	Refs.	Matrix	E [GPa]	σ_{UTS} [MPa]	Refs.
Fe	221	2427	[17]	EN AW-2099	75	305	[17]
Co	212	2799	[17]	EN AW-6056	74	411	[17]
301SS	197	2095	[25]	EN AW-6060	72	157	[26]
Haynes 25	225	1700	[26]	EN AW-6082	68	195	[25]
				AZ31	42	289	[11]

Table 3. Investigated material systems, testing frequency, und testing machine actuator used.

Material system	Testing frequency [Hz]	Testing machine actuator	Refs.
EN AW-2099 + Co	50	Servo hydraulic	[16,17]
EN AW-6056 + Fe	50	Servo hydraulic	[16,17]
EN AW-6060 + Haynes 25	30	Electro-dynamic	[15]
EN AW-6060 + 301SS	30	Electro-dynamic	[15]
EN AW-6082 + 301SS	10	Electro-dynamic	[10,12–14]
AZ31 + 301SS	10	Electro-dynamic	[10,11]

investigated composite materials (and their corresponding matrix materials) with their testing frequency and the testing machine actuator used.

4. Results

Figure 3 gives an overview of the S/N curves in double logarithmic scale for all investigated unreinforced materials and 11.1 vol% reinforced composites. The values are average values. The regression lines have been extrapolated up to the ultimate tensile strength σ_{UTS} of the particular material system (up to 0.25 cycles resp.) and up to 10^7 cycles. For all material systems, the reinforcement of 11.1 vol% leads to an increase in fatigue lifetime, which is observable by the parallel shift of the regression lines toward higher number of cycles to fracture.

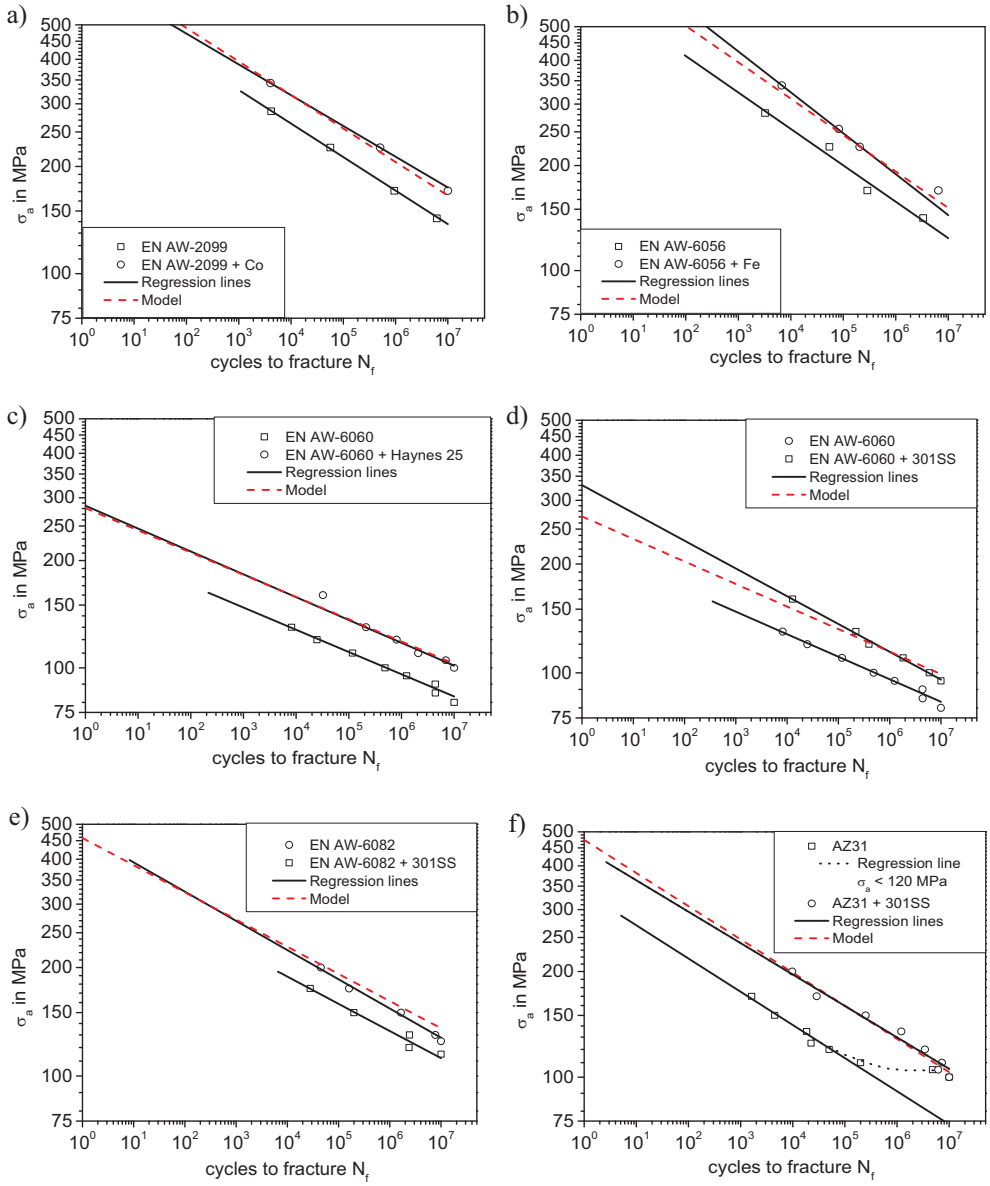

Fig. 3. S/N curves of the unreinforced materials and 11.1 vol% reinforced materials and application of the fatigue model based on Equation (5): (a) EN AW-2099 + Co,[17] (b) EN AW-6056 + Fe,[17] (c) EN AW-6060 + Haynes 25,[15] (d) EN AW-6060 + 301SS,[15] (e) EN AW-6082 + 301SS,[13] and (f) AZ31 + 301SS.[11] σ_a is the stress amplitude.

Table 4. Basquin parameters of the investigated matrix materials.

Material system	σ'_B [MPa]	b
EN AW-2099	629	–0.094
EN AW-6056	666	–0.104
EN AW-6060	227	–0.062
EN AW-6082	378	–0.076
AZ31	337	–0.095

All composite systems, except the AZ31 composite, show an additional increase in the endurance limit.

In order to apply Equation (5), Table 4 lists the Basquin parameters of the matrix materials.

The applicability of the lifetime model is also shown in Figure 3, where a very good prediction of fatigue life can be achieved for all composites.

Figure 4 compares the measured endurance limit of the composites with the calculated values. It can be summarized that the derived model also provides a relatively good prediction of the endurance limit $S_{e/10^7}$.

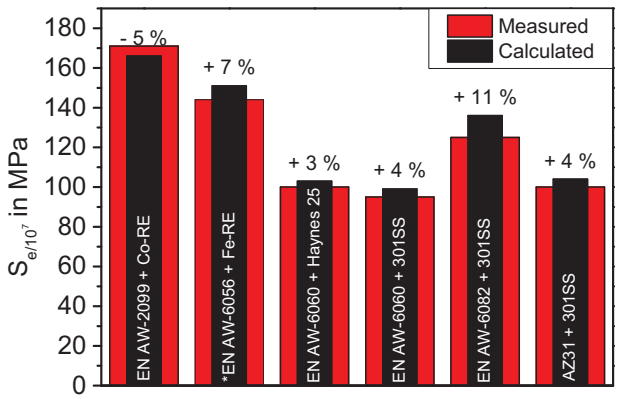

*Fig. 4. Comparison between calculated and measured endurance limit $S_{e/10^7}$ (*extrapolated value).*

5. Discussion

The results shown in the previous section attested that a volume fraction of reinforcement 11.1% leads to a significant increase of the fatigue lifetime of composite extruded lightweight materials. In order to compare the fatigue behavior of all matrix materials and all 11.1 vol% composites, Figure 5 shows the regression lines for the matrix materials (a) and the 11.1 vol% composites (b). It has to be considered that the following comparison only focuses upon the different material systems in their heat treatment states (see Table 1), whereas the influence of the different profile geometries, press ratios, and the loading frequency is not considered in detail at this point.

Figure 6 summarizes the ranking for the matrix material and the 11.1 vol% composites according to the endurance limit $S_{e/10^7}$ (a). It can be noticed that unreinforced EN AW-2099 shows a better fatigue behavior than spring steel wire reinforced EN AW-6082 and AZ31 due to the fact that this aluminum alloy is specially designed to have better fatigue resistance. The worst fatigue behavior can be attested for all EN AW-6060 material systems. Nevertheless, the advantage of reinforcements in comparison to unreinforced materials is obvious. Figure 6b shows the ranking according to the lightweight potential in terms of the specific endurance limit $S_{e/10^7}/\rho$. It can be seen that unreinforced AZ31 possesses the highest lightweight potential followed by unreinforced EN AW-2099.

Since this only focuses on the endurance limit by neglecting the fatigue behavior, Figure 7 gives an overall comparison of the fatigue behavior including all investigated unreinforced and reinforced material systems. In summary, a comparable ranking as shown in Figure 6a can be seen. Due to the different slopes (Basquin parameters), several material systems overlap at different stress amplitudes.

It can be summarized that the reinforcement leads to improved fatigue behavior in comparison to the corresponding unreinforced materials concerning a shift of the regression

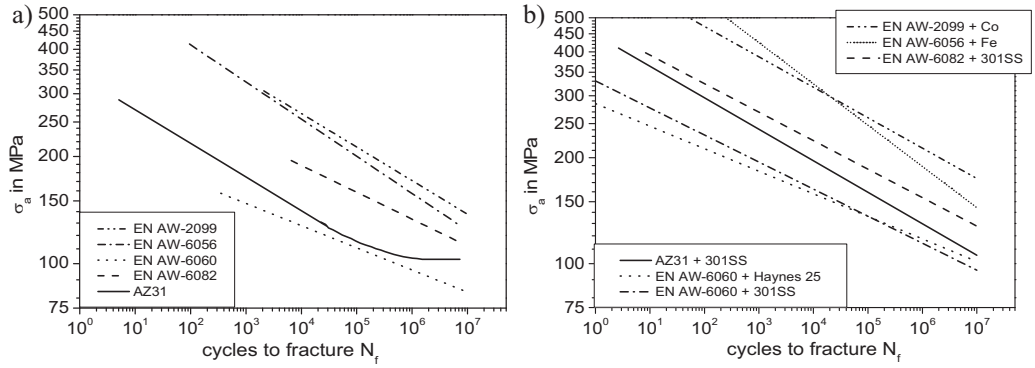

Fig. 5. S/N curves (regression lines) of all unreinforced matrix materials (a) and all 11.1 vol% reinforced composite materials (b).

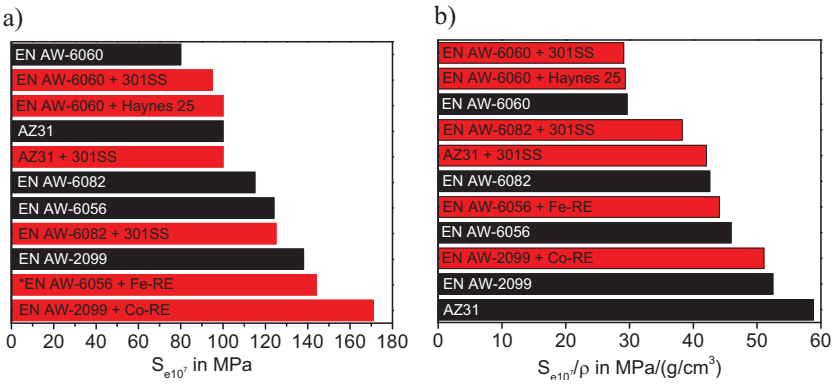

*Fig. 6. Ranking according to the best fatigue behavior in terms of the measured endurance limit $S_{e/10^7}$ (*extrapolated value) (a) and the specific endurance limit $S_{e/10^7}/\rho$ (b).*

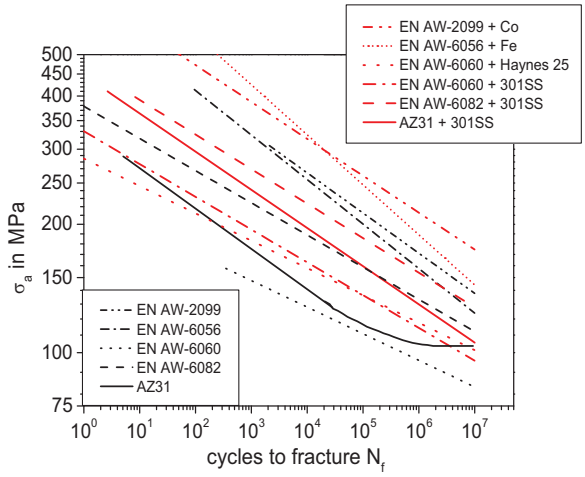

Fig. 7. S/N curves (regression lines) of all materials.

lines to higher fatigue lives as well as an increase in the endurance limit. Only for AZ31, no increase in the endurance limit can be observed (compare Figure 6).

6. Conclusions

The presented investigations showed that unidirectionally reinforced light metal alloys with a volume fraction of reinforcement 11.1% lead to significantly higher fatigue lifetimes in comparison to the single matrix material in stress controlled fatigue tests. In dependence of the matrix material used, an adequate heat treatment during the composite extrusion process leads to a vast increase of fatigue life compared to reinforced medium strong aluminum/magnesium alloys.

An innovative model, which is in good agreement with the experimental investigations, for determining of fatigue lifetime of continuous fiber reinforced metal matrix composites could be applied to other material systems with different reinforcing elements and matrix materials in different heat treatment states. The great advantage of the presented model lies in the little data needed including the quasi-static values (Young's modulus) of the single components, the volume fraction of reinforcement and the fatigue behavior of the single matrix material. A further application of this lifetime model could be the variation of the volume fraction of reinforcement as well as the verification under different *R*-ratios.

The overall comparison demonstrates that a reinforcement of lightweight materials such as hardenable aluminum alloys results in an improved fatigue behavior in comparison to the corresponding unreinforced materials.

[1] M. Kleiner, M. Schomäcker, M. Schikorra, A. Klaus, *Materialwiss. Werkst.* **2004**, *35*, 431.

[2] K. A. Weidenmann, M. Schomäcker, E. Kerscher, D. Löhe, M. Kleiner, *Light Met. Age* **2005**, *63*, 6.

[3] M. Merzkirch, K. A. Weidenmann, E. Kerscher, D. Löhe, D. Pietzka, M. Schikorra, A. E. Tekkaya, in *Materials Science and Technology (MS & T)*, Pittsburgh **2008**, p.2552–62.

[4] D. Pietzka, M. Schikorra, A. E. Tekkaya, *Adv. Mater. Res.* **2008**, *43*, 9.

[5] M. Schomäcker, M. Schikorra, M. Kleiner, *4 Years of Research on Composite Extrusion for Continuous Reinforcement of Aluminium Profiles, 6th Aluminium Two Thousand World Congress*, Florence, Italy **2007**.

[6] D. Pietzka, N. B. Khalifa, S. Gerke, A. E. Tekkaya, *Key Eng. Mater.* **2013**, *554–557*, 801.

[7] A. A. Baker, *J. Mater. Sci.* **1968**, *3*, 412.

[8] B. Moser, L. Weber, A. Mortensen, *Scr. Mater.* **2005**, *53*, 1111.

[9] D. Bettge, B. Günther, W. Wedell, P. D. Portella, J. Hemptenmacher, P. W. M. Peters, B. Skrotzki, *Mater. Sci. Eng.* **2007**, *A452–453*, 536.

[10] M. Merzkirch, A. Reeb, K. A. Weidenmann, A. Wanner, V. Schulze, *J. Acoust. Emission* **2011**, *29*, 317.

[11] M. Merzkirch, K. A. Weidenmann, V. Schulze, *Int. J. Fatigue* **2013**, *56*, 60.

[12] K. A. Weidenmann, E. Kerscher, M. Merzkirch, *Adv. Eng. Mater.* **2010**, *12*, 637.

[13] M. Merzkirch, A. Reeb, K. A. Weidenmann, V. Schulze, *J. Mater. Sci.* **2014**, *49*, 2187.

[14] M. Merzkirch, *Dissertation am Karlsruher Institut für Technologie (KIT)*, Institut für Angewandte Materialien (IAM), KIT Scientific Publishing, Karlsruhe **2012**, ISBN 978–3-86644–933–6.

[15] K. A. Weidenmann, Th. Schwind, E. Kerscher, D. Löhe, *Materialwiss. Werkst.* **2007**, *38*, 75.

[16] K. A. Weidenmann, E. Kerscher, T. Hammers, *Adv. Eng. Mater.* **2010**, *12*, 584.
[17] T. Hammers, *Dissertation am Karlsruhe Institut für Technologie (KIT)*, Institut für Angewandte Materialien (IAM), KIT Scientific Publishing, Karlsruhe **2013**, ISBN: 978–3-86644–947–3.
[18] Z. R. Xu, K. K. Chawla, A. Wolfenden, A. Neuman, G. M. Liggett, N. Chawla, *Mater. Sci. Eng.* **1995**, *A203*, 75.
[19] B. S. Majumdar, G. M. Newaz, *Mater. Sci. Eng.* **1995**, *A200*, 114.
[20] R. Talreja, *Mater. Sci. Eng.* **1995**, *A200*, 21.
[21] W. Voigt, *Abh. Kgl. Ges. Wiss. Göttingen Math.* **1887**, *K134*, 3.
[22] A. Kelly, J. Davies, *Metall. Rev.* **1965**, *10*, 1.
[23] O. H. Basquin, *Proc. ASTM* **1910**, *10*, 625.
[24] T. Kloppenborg, T. Hammers, M. Schikorra, E. Kerscher, E. A. Tekkaya, *Adv. Mater. Res.* **2008**, *43*, 167.
[25] M. Merzkirch, M. Meissner, V. Schulze, K. A. Weidenmann, *J. Compos. Mater.* **2014**, *49*, 261.
[26] K. A. Weidenmann, E. Kerscher, V. Schulze, D. Löhe, *Adv. Mater. Res.* **2006**, *10*, 23.